Fourier-Transform Infrared Spectroscopy Study of Dioleoylphosphatidylcholine and Monooleoylglycerol in Lamellar and Cubic Liquid Crystals[†]

Anders Nilsson, Allan Holmgren,* and Göran Lindblom
Department of Physical Chemistry, University of Umeå, S-901 87 Umeå, Sweden

Received July 26, 1990; Revised Manuscript Received October 8, 1990

ABSTRACT: The liquid-crystalline phases of the systems monooleoylglycerol (MO)/water, dioleoylphosphatidylcholine (DOPC)/water, and MO/DOPC/water have been studied by Fourier–transform infrared (FTIR) spectroscopy. In the latter ternary system, the *sn*-3 OH group of MO competes with water to interact with the polar head group of DOPC, and an intramolecular hydrogen bonding of MO is broken up. The hydration of the ester carbonyl groups in the lamellar phases of both the MO/water and DOPC/water systems increases with increasing water content. Similarly, the addition of small amounts either of MO to a DOPC/water system or of DOPC to an MO/water system also results in an increase in the hydration of the ester carbonyl groups. This leads to an unfavorable hydrocarbon–water contact which is counteracted by the formation of a cubic phase, except for the DOPC/water system, where the lamellar phase is stable also at the highest water concentrations. The phase behavior of the different systems can be described in terms of lipid monolayer curvature and molecular packing in the lipid aggregates. Finally, it is shown by the water association band in the FTIR spectrum that the water hydrogen bonding is considerably different in the liquid-crystalline phases than in bulk water.

Phospholipids and acylglycerols are amphiphilic molecules abundantly occurring in biological systems, where they to a large extent are involved in the building up of different aggregate structures. Among these, the lipid bilayer has been subjected to an overwhelming number of physicochemical studies. In recent years, it has become evident that such lipids also may form other structures than the common membrane bilayer. Thus, it has been shown that many of the biological lipids dispersed in water may form reversed hexagonal (H_{II})[1] phases and various isotropic cubic liquid-crystalline phases (Lindblom & Rilfors, 1989; Seddon, 1990). Although a typical membrane lipid by itself in water forms a thermodynamically stable lamellar liquid-crystalline (L_α) phase, it is often possible to accomplish a phase transition to a nonlamellar phase by changing composition, temperature, pressure, etc. For example, addition of alkanes or hydrophobic peptides may induce an H_{II} phase in phosphatidylcholines (Sjölund et al., 1987, 1989; Lindblom et al., 1988), and it has also been shown that alkanes decreases the L_α to H_{II} phase transition temperature for phosphatidylethanolamines (Gruner, 1989; Siegel et al., 1989). Likewise, a mixture of membrane lipids may form nonlamellar structures in water. Investigations (Wieslander et al., 1981; Kahn et al., 1981; Lindblom et al., 1986) of the phase behavior of the membrane lipids from *Acholeplasma laidlawii* show that one of the glucolipids, monoglucosyldiacylglycerol (MGDG), plays an important role in the regulations of the membrane lipid composition by its tendency to form nonlamellar phase structures. Furthermore, enzyme activity may strongly depend on the presence of a lipid forming nonlamellar phases (Navarro et al., 1984; Jensen & Schutzbach, 1984, 1988, 1989).

Monoacylglycerols like monoolein (MO) are involved in fat digestion occurring in the upper small intestine (Patton & Carey, 1979). During this process, a number of different liquid-crystalline phases are formed as, for example, lamellar and cubic phases. Since the lipases perform their enzymatic reaction with highest efficiency at the water/hydrocarbon interface of a lipid bilayer, it has been speculated (Lindblom & Rilfors, 1989) that a bicontinuous cubic phase built up by lipid bilayers might constitute a suitable matrix for the enzymatic process. It should be noted that MO is highly potent in inducing a cubic phase in phospholipid systems (Gutman et al., 1984), which can be taken as further support for these ideas. Furthermore, MO is known to be a very effective fusogenic lipid (Hope & Cullis, 1981), again supporting the suggestion that the phase behavior of certain lipids is essential for some biological processes [see also Lindblom and Rilfors (1989)].

In many respects, the phase behavior presented by MO itself and in mixtures with membrane lipids is providing us with excellent model membrane systems for physicochemical investigations of structures, dynamics, and lipid–lipid interactions. The binary phase diagram of MO and water was determined by Lutton (1965). The most striking property in this diagram is perhaps that a bicontinuous cubic phase is in equilibrium with water (cf. Figure 1). Recently, it was shown that there are two cubic phases [belonging to the space groups *Pn3m* (Longley & McIntosh, 1983) and *Ia3d* (Hyde et al., 1984)] in equilibrium with each other. The larger part of the ternary phase diagram of the system dioleoylphosphatidylcholine (DOPC), MO, and water has also been determined (Gutman et al., 1984). This diagram exhibits a large nonlamellar phase area representing a bicontinuous cubic phase (Figure 1) and also a smaller area at low water content, where an H_{II} phase is present. Cubic phases are also obtained with mixtures of DPPC/MO and with DPPE/MO (Tilcock & Fisher, 1982).

[†] This work was supported by the Swedish Natural Science Research Council.

[1] Abbreviations: DOPC, dioleoylphosphatidylcholine; MO, monooleoylglycerol; MGDG, monoglucosyldiacylglycerol; PA, phosphatidic acid; PC, phosphatidylcholine; PE, phosphatidylethanolamine; DO, dioleoyl; DP, dipalmitoyl; FTIR, Fourier-transform infrared; NMR, nuclear magnetic resonance; H_{II}, reversed hexagonal phase; L_α, lamellar phase; H_0, spontaneous curvature.

0006-2960/91/0430-2126$02.50/0

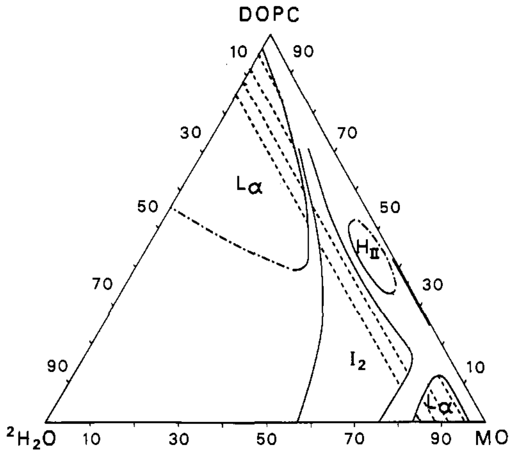

FIGURE 1: Tentative ternary phase diagram for the system MO/DOPC/water at 28 °C. L_2, isotropic phase; H_{II}, reversed hexagonal liquid-crystalline phase ; I_2, bicontinuous cubic liquid-crystalline phase; L_α, lamellar liquid-crystalline phase. The compositions of the samples studied in this work are located along the indicated dashed lines.

In our previous work on acylglycerols, we have studied sodium and cesium ion binding and water interaction by ^{23}Na, ^{133}Cs, and ^{2}H NMR (Lindblom et al., 1978; Persson & Lindblom, 1979), the water and lipid lateral diffusion in lamellar and cubic phases (Lindblom & Wennerström, 1977; Lindblom et al., 1979), and the ordering of guest molecules in macroscopically aligned bilayers by linear dichroism with polarized UV (Johansson et al., 1978, 1979, 1981; Johansson & Lindblom, 1980, 1981) and IR light (Holmgren et al., 1987), and recently Fourier-transform infrared (FTIR) spectroscopy was used in the study of the intramolecular hydrogen bonding in a monoacylglycerol system (Holmgren et al., 1988). In recent years, many lipid systems have been studied by FTIR in order to determine, e.g., critical micelle concentrations, phase transition temperatures, acyl chain conformation, etc. (Mantsch et al., 1980, 1981; Umemura et al., 1980, 1981; Kawai et al., 1984; Mendelsohn et al., 1984). The importance of lipid intermolecular hydrogen bonding for the structure and organization in membranes has been reviewed by Boggs (1987). Although the evidence for this kind of hydrogen bonding still must be considered as weak, there are experimental studies that give indirect support [see Boggs (1987)]. The lifetime of hydrogen bonds in water is of the order of 10^{-11} s, and it seems reasonable to assume that the lifetime of an intermolecular hydrogen bond between lipids in an aggregate is of a similar order of magnitude. Therefore, these hydrogen bonds are rapidly broken and re-formed between the lipid molecules in the aggregates and between water molecules on the surface surrounding the aggregate. Protons can, for example, be transported laterally along a phosphatidylethanolamine (PE) monolayer with a velocity which is about 20 times faster than in bulk water (Teissie et al., 1985; Tocanne & Teissie, 1990). There are also theoretical studies (Berde et al., 1980; Nagle, 1980) which indicate that hydrogen bonding between the lipid head groups is to some extent responsible for the high transition temperature between the gel and the L_α phases for PE and phosphatidic acid (PA). Thus, although the hydrogen bonds of lipid head groups are not long lasting, they may stabilize a particular lipid arrangement, which in turn might determine the aggregate structure formed. It is therefore suggested that hydrogen bonds should be explicitly included in the theoretical models describing phase transitions between membrane lipid structures. In this work, FTIR spectroscopy has been utilized to delineate the importance of the hydrogen bonding between lipid head groups in a system containing DOPC and MO, where the polymorphism is rather rich (Figure 1). The study is aimed at acquiring a better understanding of the possible influence of hydrogen bonding in the phase transitions between the L_α, cubic, and H_{II} phases. The data obtained are discussed in terms of molecular packing in the different phase structures formed and the changes in the geometrical shape of the lipid molecules upon a phase transition or equivalently in terms of changes in the lipid monolayer curvature of the aggregate.

MATERIALS AND METHODS

The lipids were purchased from Avanti Polar Lipids Inc. (DOPC) and Sigma Chemical Co. (MO) and were used without further purification. The liquid-crystalline samples were prepared with water from a Millipore system. The samples were dried in high vacuum (10^{-6} mmHg) for at least 72 h and prepared by weighing, and the sample tubes were then sealed. Sample homogeneity was ensured by centrifuging the samples at 5000*g*. The compositions of the sample studied are located along the dashed lines in Figure 1. Spectra were recorded with a Bruker IFS 113V FTIR spectrometer, equipped with a liquid nitrogen cooled MCT detector. Teflon spacers from Specac Instrument were used to vary the path length between the CaF_2 windows (6–250 μm). The temperature of the CaF_2 plates was kept within ±0.05 °C in the temperature range 25–65 °C. A total of 512 scans were combined, and the resultant interferogram was Fourier-transformed to obtain a resolution of 2 cm^{-1} over the spectral range. In the study of band contours comprised of more than one component, a deconvolution technique was used along with band simulation. The observed band contour was calculated from a superposition of components that were either Gaussian, Lorentzian, or a combination of these two line shapes.

RESULTS AND DISCUSSION

In the FTIR spectrum, a change in a particular interaction is detected as a frequency shift for the specific vibrational mode or as a change in the line shape (Pimentel & McClellan, 1960). Discrete frequency ranges in the spectrum can be assigned to different parts of the lipid molecule (head group, methylene group, etc.), and, therefore, detailed information about the molecular interactions can be obtained. Thus, the phosphate stretching modes occur in the frequency domain 1000–1300 cm^{-1} (the symmetric mode $\bar{\nu}_s$–PO_2^- at 1088 cm^{-1} and the antisymmetric mode $\bar{\nu}_a$–PO_2^- at 1240 cm^{-1}, and in the same spectral range are the *sn*-1 CO–O–C antisymmetric stretching (1180 cm^{-1}), the *sn*-2 C–OH stretching (1120 cm^{-1}), and the *sn*-3 C–OH stretching (1050 cm^{-1}) modes of MO. The carbonyl stretching mode $\bar{\nu}$—C═O is observed in the range 1600–1800 cm^{-1}. The methylene modes are found at about 2850 cm^{-1} (symmetric stretching) and at about 1470 cm^{-1} (scissoring). Since the methylene peaks are unaltered for the phase transitions between the liquid-crystalline phases investigated here, we will not discuss these spectral peaks any further. However, it should be noted that upon a phase transition between the gel and the L_α phases, there is a frequency shift observed of the methylene peaks due to the large change in the acyl chain conformation (Casal & Mantsch, 1984). It can therefore be concluded that the acyl chain conformation is very similar in the different liquid-crystalline phase structures, as seen by FTIR. The order parameter profiles determined by ^{2}H NMR, on the other hand, suggest that there is a slight difference in the acyl chain conformation in the L_α and H_{II} phases (Sternin et al., 1988; Turmond & Brown, 1991). This apparent discrepancy may be due to the resolution in the FTIR measurements (2 cm^{-1}), since, e.g., the

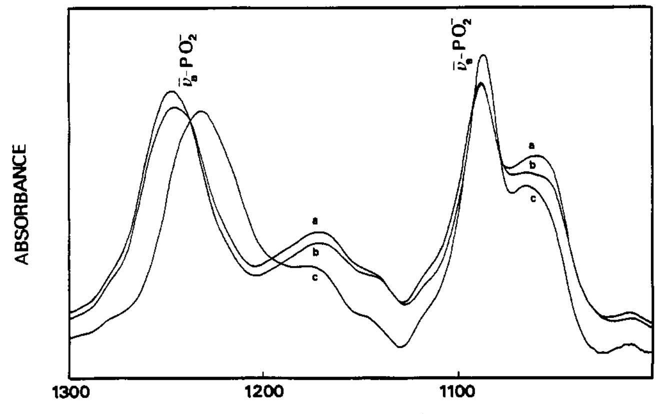

FIGURE 2: Infrared spectra of the phosphate vibrational modes of DOPC/water: (a) 5% water at 25 °C; (b) 5% at 65 °C; (c) 20% water at 25 °C. Concentrations are given in weight percentage.

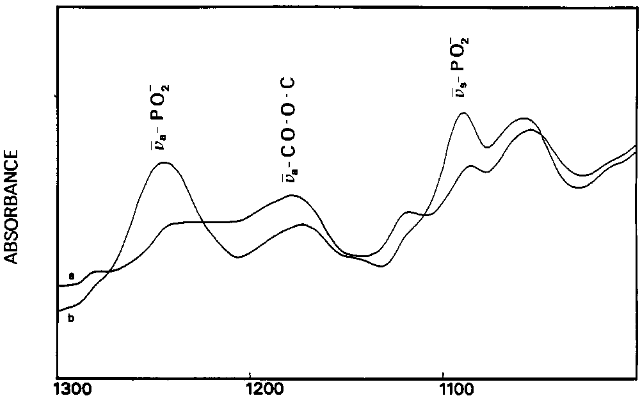

FIGURE 3: Infrared spectra of the phosphate vibrational mode region. (a) Experimental spectrum of DOPC/MO/water (44/44/12%) and (b) the corresponding linear-combined calculated spectrum. Concentrations are given in weight percentage.

difference in the frequency shift of the CH_2 band is only 3 cm^{-1} for lipid monomer and micellar solutions. Finally, a so-called association (combination) band of water is found in the spectral range 1900–2300 cm^{-1}, and the stretching modes of OH groups are observed in the frequency domain 3000–3700 cm^{-1}.

Stretching Modes at 1000-1300 cm^{-1} (PO$_2^-$, CO-O-C, C-OH)

DOPC/Water. An increase of the water concentration in the L_α phase gives rise to a decrease in the frequency of the $\bar{\nu}_a$–PO$_2^-$ peak (Figure 2). The frequency shift is about 15 cm^{-1} when the water content is varied between 5 to 20 wt %. Likewise for a sample with 5 wt % water, a change in the temperature from 25 to 65 °C leads to an increase of the frequency by about 9 cm^{-1} of this peak. These findings strongly indicate a formation of hydrogen bonds between water and the phosphate head groups of DOPC (Pimentel & McClellan, 1960). This conclusion is also in agreement with previous findings that the hydration of DOPC is as high as 11 water molecules per lipid (Finer & Darke, 1974). The peak frequency of the symmetric $\bar{\nu}_s$–PO$_2^-$, on the other hand, is only slightly affected by the interaction between the water molecules and the phosphate groups. Here the frequency shift amounts to only about 3 cm^{-1} for a change in the water content from 5 to 20 wt %, while the intensity of this peak relative to the peak frequency of the $\bar{\nu}_a$–PO$_2^-$ mode increases considerably with increasing water content (Figure 2). This change in intensity may be due to a change in the molecular ordering of the phosphate groups (Holmgren et al., 1987).

MO/Water. A change in the water concentration of the lamellar phase from 5 to 15 wt % (corresponding to the molar ratios MO/H_2O 1/1.0 and 1/3.5) had no influence on the frequency of the *sn*-3 C–OH stretching mode at 1050 cm^{-1}, and it should be noted that the peak frequency is the same as that for MO in a CCl_4 solution. It can therefore be concluded, as discussed in a previous report (Holmgren et al., 1988), that the *sn*-3 OH group forms an intramolecular hydrogen bond to the ester carbonyl group of MO. For the $\bar{\nu}_a$–CO–O–C mode, there is an increase by 5 cm^{-1} in the frequency upon a water increase. This is somewhat unexpected, since a stretching mode usually shifts toward lower frequency with increasing polarity in the surroundings of the vibrational entity. A possible interpretation of this finding might be that a structural rearrangement of the polar head group occurs with increasing hydration.

DOPC/MO/Water. The addition of a small amount (about 2 wt %) of MO to a lamellar phase of DOPC/water gives rise to significant changes in the $\bar{\nu}_a$–PO$_2^-$ peak at 1240 cm^{-1}. Thus, the width of the band increases, the intensity decreases, and there is a shift toward lower wavenumbers (2–3 cm^{-1}). These changes are further reinforced with increasing MO content, and for a cubic liquid-crystalline phase, composed of a 50–50 wt % mixture of DOPC and MO (corresponding to a molar ratio of 1/2.2), the $\bar{\nu}_a$–PO$_2^-$ peak has nearly disappeared. In order to get information about whether the observed changes in the spectrum are due to interactions between the phosphate group and the MO head groups, a linear combination of spectra from a pure DOPC/water and a pure MO/water system was performed with the computer of the FTIR spectrometer (Figure 3). As can be inferred from this figure, there is no resemblance between the measured and the linear combined spectra, indicating that there are interactions between DOPC and MO in the liquid-crystalline phases investigated. It should be noted that neither the broadening nor the shift of the peak at 1240 cm^{-1} can be due to any vibrational modes of MO, since MO has virtually no absorption in this spectral region.

The addition of a small amount of DOPC to a lamellar phase of MO/water has no effect on the *sn*-2 C–OH stretching mode of MO but affects the *sn*-3 C–OH stretching mode. A small shift (2 cm^{-1}) toward a lower wave number is obtained at a molar ratio of 1/10 between DOPC and MO.

Taken together, all these findings indicate that for a mixture of DOPC and MO there is an interaction between these molecules at the aggregate interface (the surface of the lipid monolayer). In the lamellar phase of the MO/water system, the *sn*-3 C–OH forms an intramolecular hydrogen bond to the carbonyl group, which by addition of DOPC is broken and hydrogen bonding between the hydroxylic group(s) of MO and the phosphate group of DOPC begins to form.

Carbonyl Absorption at 1600-1800 cm^{-1}

DOPC/Water. The infrared absorption of the two ester carbonyls of DOPC has its intensity maximum at 1735 cm^{-1} (Figure 4a). In the past 10 years, carbonyl groups of phospholipids have been subject to several infrared and Raman spectroscopic studies (Bush et al., 1980; Blume et al., 1988; Wong et al., 1988). In the FTIR study by Wong et al. (1988), it was concluded that the 1746.7 cm^{-1} band of a dimyristoylphosphatidylcholine aqueous dispersion can be unambiguously attributed to the $\bar{\nu}$—C=O of the *sn*-1 carbonyl group and that the two bands observed at 1735.8 and 1726.6 cm^{-1} are caused by free and hydrogen-bonded *sn*-2 C=O groups. For samples with excess water, only these two latter

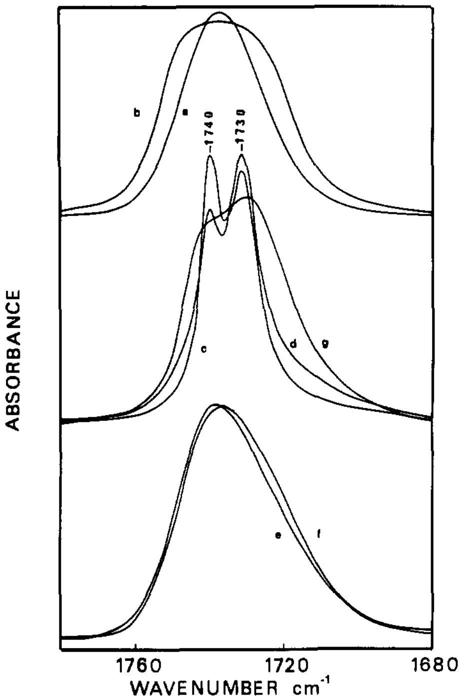

FIGURE 4: Infrared spectra of the carbonyl stretching modes in samples of (a) DOPC and 8% H_2O, (b) DOPC and 8% H_2O and 4% MO, (c) MO and 8% H_2O, (d) MO and 8% H_2O and 4% DOPC, (e) DOPC/MO/water (42.5/42.5/15%) (cubic phase), (f) the same as in (e), but a linear combination of spectra from a pure DOPC/water and a pure MO/water system, and (g) MO and 30% H_2O (cubic phase). Concentrations are given in weight percentage.

bands could be resolved. Blume et al. (1988), on the other hand, claim in a study by using specifically ^{13}C-labeled C=O groups of the phospholipids that both the *sn*-1 and the *sn*-2 C=O groups give rise to two bands corresponding to free and hydrogen-bonded carbonyl groups.

For the lamellar liquid-crystalline phase of DOPC/water in this investigation, a single band at 1735 cm^{-1} is observed (Figure 4a), indicating that the two C=O groups are located in similar environments. However, as can be seen in Figure 4, the band profile is asymmetric, having a slightly larger intensity on the low-frequency side of the peak. This asymmetry increases with increasing water concentration, while the C=O stretching band does not change its peak maximum. Furthermore, when an intrinsic Lorentzian line shape was used, this band could not be deconvoluted into two component bands, and it should be noted that a 10^{-2} M solution of DOPC in CCl_4 also exhibits an asymmetric C=O band, having larger intensity on the low-frequency side of the peak. These experimental findings instead suggest that reorientational and/or vibrational relaxation of the two C=O vibrators is causing the line shape of the 1735 cm^{-1} band. Therefore, the information obtained from this band must be discussed in terms of dynamics rather than of structure.

MO/Water. The carbonyl absorption band of MO for a lamellar (8 wt % H_2O) and a cubic (30 wt % H_2O) phase exhibits two clearly separated peak maxima at 1730 and 1740 cm^{-1} (Figure 4c,g), in spite of the fact that there is only one C=O group in the MO molecule. Recently, the peak observed at 1730 cm^{-1} was attributed (Holmgren et al., 1988) to intramolecular hydrogen bonding.

MO/DOPC/Water. The addition of DOPC to a *lamellar* sample of MO/water leads to that the two C=O bands gradually coalesce into eventually one peak, accompanied by a large symmetric broadening (Figure 4c,d,e). Thus, at low DOPC contents, two C=O peaks are still observed, but the width at half-height of the peaks has increased (Figure 4c,d), and the peak absorbance at 1730 cm^{-1} appears to increase in intensity at the expense of the absorbance at 1740 cm^{-1}. This again strongly indicates that the OH group(s) of MO interact(s) with the polar head group (phosphate and/or ester carbonyls) of DOPC. The observed broadening of the C=O stretching band may be due to a vibrational dephasing mechanism (Rothschild, 1984), where water would give a broader distribution of vibrational energy levels. This will lead to an increasing perturbation of the C=O stretching mode, which is also in line with the experimental observation that the broadening of the C=O band increases with increasing water concentration. Thus, addition of DOPC to the MO/water system facilitates the interaction between water molecules and the ester carbonyl groups at the interfacial region of the lipid aggregates.

At low concentration (4 wt %) of MO in the lamellar phase of the system DOPC/MO/water, the C=O stretching band broadens considerably, while the peak maximum remains at 1735 cm^{-1} (Figure 4a,b). The width at half-height of this band is 36 cm^{-1}, a similar value (34 cm^{-1}) of which was also obtained for this band of DOPC in $CHCl_3$ solution. In this latter solvent, the C=O groups are hydrogen bonded to $CHCl_3$. For the DOPC/water and MO/water systems, the widths at half-height of the C=O stretching band are 25 and 18 cm^{-1}, respectively. These results strongly indicate that hydrogen bonding is involved in the interactions occurring at the interfacial region of the lipid aggregate, giving further support for the water interactions with the ester carbonyl group.

The width at half-height of the C=O band in the *cubic* phase of the DOPC/MO/water system is considerably smaller than in the lamellar phase. This pertains for samples containing even small amounts of MO (cf. Figure 4b,e). Furthermore, the intensity on the low-frequency side of the C=O absorption band in the cubic phase is much lower than in the lamellar phase. These results strongly indicate that the C=O group is less hydrated in the cubic phase than in the lamellar phase. In order to further elucidate the effect on the C=O stretching vibration at the phase transition between the lamellar and the cubic phases, a linear combination of spectra was performed from an MO/water lamellar phase (12 wt % H_2O) spectrum and a DOPC/water lamellar phase (12 wt % H_2O) spectrum. Note that a mixture of these two lamellar phase samples will result in the formation of a cubic phase (cf. Figure 1). The calculated spectrum, having a DOPC/MO molar ratio of 1/2.2, is shown in Figure 4f, which can be compared with the experimental spectrum of the corresponding cubic phase shown in Figure 4e. Thus, the measured C=O stretching band is narrower than the calculated one, and the characteristic absorption at 1730 cm^{-1} appears as a shoulder in the calculated spectrum, while it has vanished in the measured one. Most probably, this difference in the line shape of the C=O peak at this phase transition is due to a disruption of the intramolecular hydrogen bonding of MO, again supporting the interpretation given above.

Water Absorption at 2000–2600 cm^{-1}

In this spectral region, the so-called association (combination) band of water is observed. This band has been assigned to the transition $\bar{\nu}_2+\bar{\nu}_R$, where $\bar{\nu}_2$ is the bending mode and $\bar{\nu}_R$ is a librational mode (Lutz et al., 1978). The advantage of using this spectral region when examining water in liquid-crystalline phases is that only water absorbs light in this frequency domain. This offers an interesting possibility to investigate water–lipid interactions. The association band of liquid water is shown in Figure 5a. This band is clearly

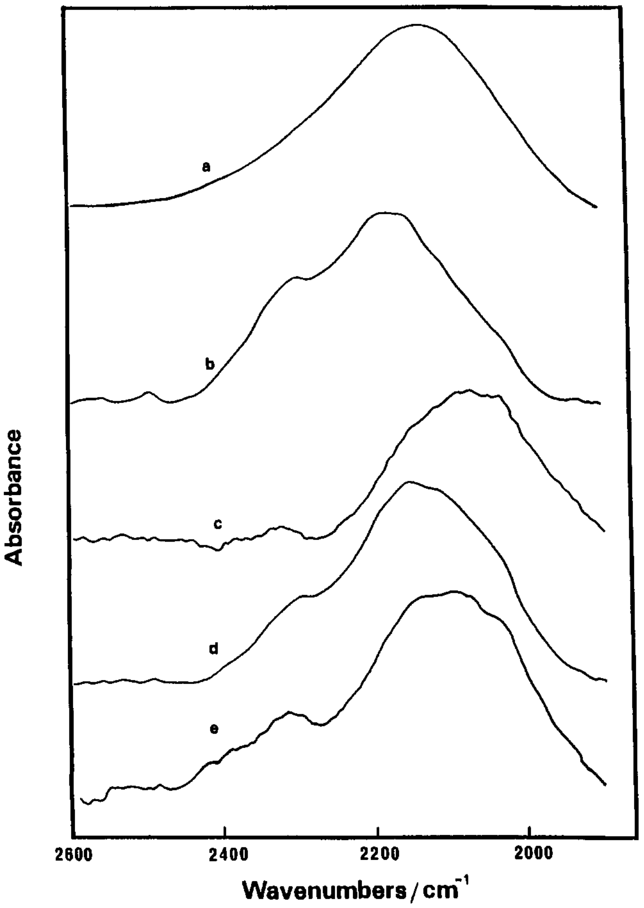

FIGURE 5: Infrared spectra of the association band of water at 25 °C; (a) pure water; (b) DOPC and 12% water (lamellar phase); (c) MO and 12% water (lamellar phase); (d) DOPC/MO/water, 44/44/12% (cubic phase), and (e) linear combination of spectra from a pure DOPC/water and a pure MO/water system (12% water). Concentrations are given in weight percentage.

affected by the addition of MO and/or DOPC (Figure 5b,d).

DOPC/Water. The spectral feature of the association band of water ($\bar{\nu}_{\mathrm{assn}}$–$H_2O$) depends on the lipid/water ratio. At high water concentration (≃30 wt %), the spectrum is very similar to a spectrum of liquid water. According to other investigations, the lecithin head group is capable to bind 12–13 water molecules which corresponds to a water concentration of about 20 wt % (McIntosh et al., 1986; LeNeveu et al., 1977). Below this value, we therefore expect to observe only water molecules that interact with the head-group region of the lipid molecules. In Figure 5, a spectrum of liquid water (a) and a spectrum of water in DOPC (12 wt % water, b) are shown. Important changes in band shapes, peak maxima, and relative intensities occur. The peak position of $\bar{\nu}_{\mathrm{assn}}$–$H_2O$ at 2128 cm^{-1} (pure H_2O) shifts to higher frequency in the DOPC/water mixture, and a band with an intensity maximum at 2306 cm^{-1} appears. It is well-known that OH bending vibrations increase in frequency when the hydroxyl group participates in a hydrogen bond. Therefore, the shift of the peak position to higher frequency indicates stronger hydrogen-bonded water molecules as compared with the situation in bulk water. However, it is known from the literature that the frequency of OH bending modes only increases some 10 or 20 wavenumbers upon hydrogen-bonding formation. We therefore suggest that the association band is strongly influenced by the librational modes of water and that the frequency of these modes increases as the water molecule is subjected to a stronger interaction. The line shape of $\bar{\nu}_{\mathrm{assn}}$–$H_2O$ suggests several shoulders. However, the band at 2306 cm^{-1} is clearly resolved, and there exists at least two distinctly different environments for water molecules in the DOPC/water system, giving rise to two bands with peak positions at about 2170 and 2306 cm^{-1}. The intensity of the band with maximum intensity at 2170 cm^{-1} decreases with decreased water concentration, but the intensity and frequency of the band at 2306 cm^{-1} are nearly unchanged down to about 3 wt % water in DOPC. However, at a water concentration below 3 wt % the 2306 cm^{-1} band starts to lose intensity. As the intensity is proportional to the concentration of the absorbing species, this behavior of the association band also indicates two different "types" of water. From an X-ray investigation (Pearson et al., 1979), it was suggested that a DOPC molecule has one water molecule located at the phosphate group and that this water molecule is so strongly bound that it is hard to remove. One water molecule corresponds to 2.6 wt % water in a DOPC/water system. Therefore, we assign the band with maximum intensity at 2306 cm^{-1} to water molecules, strongly hydrogen-bonded to the negatively charged phosphate group of DOPC.

MO/Water. The water association band has a considerably smaller bandwidth for the MO/water samples than for bulk water, and the peak position is shifted to 2090 cm^{-1}, i.e., about 40 cm^{-1} toward lower frequency (Figure 5c). Thus, water between MO bilayers is severely perturbed compared with bulk water (Figure 5a,c), since a shift of the peak position toward lower wavenumbers indicates that the hydrogen bonds of the water molecules are diminished. Thus, for both the MO/water and the DOPC/water systems, the FTIR spectrum is sensitive to the anisotropic environment felt by the water molecules in the lyotropic liquid-crystalline phases.

MO/DOPC/Water. Addition of MO to the DOPC/water system gives rise to a decrease in the 2306 cm^{-1} band (Figure 5d). A linear combination of the spectra in Figure 5b (DOPC/water, L_α phase) and Figure 5c (MO/water, L_α phase) is shown in Figure 5e. It can be inferred from the latter figure that besides a lower intensity at 2306 cm^{-1}, the measured spectrum (Figure 5d) has its maximum peak at significantly higher frequency. The decrease in the intensity at 2306 cm^{-1} suggests that there is a decrease in the number of water molecules, strongly hydrogen-bonded to the PO_2^- group of DOPC, which seems to be reasonable if the hydroxylic groups of MO are competing with water in the hydration of the PO_2^- group. The shift of the maximum intensity toward a higher frequency, on the other hand, strongly indicates that more water is bound to the polar head group of DOPC in the DOPC/MO/water system than to that of MO.

OH Stretching Region at 3000–3700 cm^{-1}

The infrared spectrum of liquid water exhibits a broad, poorly resolved spectral feature in the hydrogen-bonding range (Figure 6a). This band consists of subbands (Zundel, 1969; Sarikov et al., 1974) assigned to the stretching vibration of the "non-hydrogen bonded" OH groups (3615 cm^{-1}), to hydrogen-bonded OH groups (3420 cm^{-1}; it should be noted that this band should consist of symmetric and antisymmetric stretching modes), and to the overtone of the symmetric bending vibration of the water molecules (3250 cm^{-1}). In the following, it is convenient to use the spectrum of liquid water as a reference state. For water molecules forming stronger hydrogen bonds than in bulk water, the stretching vibrational modes are shifted toward a lower frequency.

DOPC/Water. It can be inferred from Figure 6 that water is clearly affected by the presence of DOPC. The intensity maximum of the OH band shifts about 20 cm^{-1} toward lower frequency, indicating stronger hydrogen-bonded water mole-

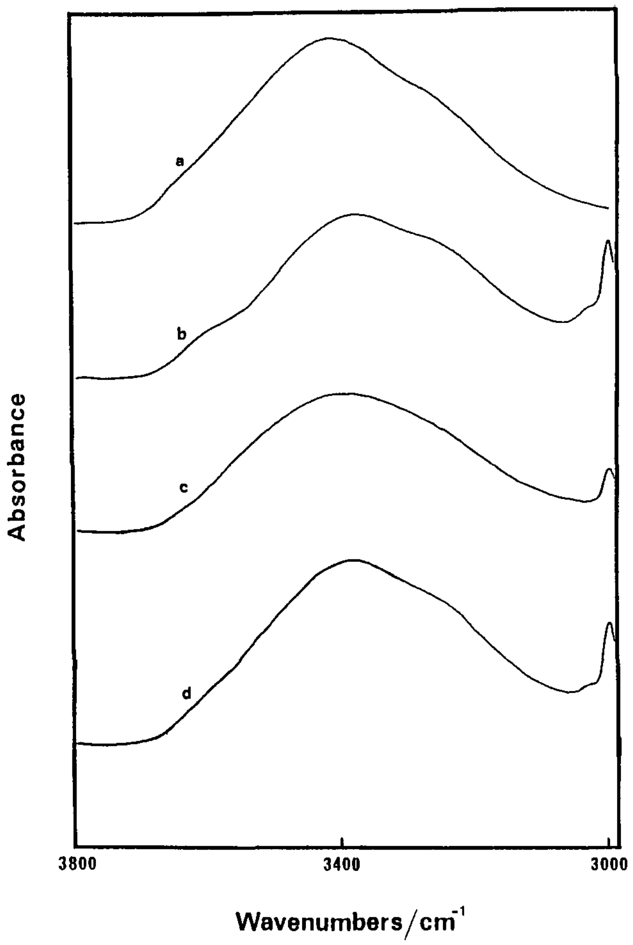

FIGURE 6: Infrared spectra of the OH stretching region for (a) pure water, (b) DOPC and 15% water, (c) MO and 15% water, and (d) DOPC/MO/water with the composition 42.5/42.5/15%. Concentrations are given in weight percentage.

cules than in bulk water. This is consistent with the spectral behavior observed in the 1000–1300 and 2000–2600 cm^{-1} regions. The shoulder at 3615 cm^{-1} is more distinct in DOPC/water than in bulk water.

MO/Water. The OH band of a lamellar phase in the MO/water system (Figure 6c) is complicated by the presence of the OH groups from MO itself. The OH band of dry MO has its maximum intensity at 3270 cm^{-1}, but unfortunately a subtraction of this band from the spectrum of the MO/water system is somewhat ambiguous, since it can be expected that the hydrogen bonding in the MO/water system is different from that in a pure MO system. However, a digital subtraction of the OH band of dry MO from the spectrum of an MO/water system results in a reduced intensity on the low-frequency side of the OH band in Figure 6c, implying that the width at half-height of the OH band is diminished and the peak position is shifted toward higher wavenumber than in bulk water. This indicates weaker hydrogen bonding and more dynamically restricted water in the liquid-crystalline phase than in the bulk water, which is in agreement with the spectral observations for the MO/water system in the 2000–2600 cm^{-1} region.

DOPC/MO/Water. The spectrum of the cubic liquid-crystalline phase of DOPC/MO/water (42.5/42.5/15 wt %) shown in Figure 6d, has a band profile rather similar to the spectrum of bulk water. However, the relative intensity at 3270 cm^{-1} is higher, as expected if the hydroxyl groups of MO have their peak frequency at that wavenumber. Furthermore, the width of the hydroxyl band in Figure 6d is considerably narrower than the width of the liquid water spectrum. Thus, it follows that water molecules in the cubic phase are subjected to a narrower range of interactions than they are in bulk water.

Head-Group Interaction and Phase Behavior

In recent years, much work has been devoted to get a better understanding of the self-assembly of lipids and their phase behavior. The theoretical models used, although still rather crude and qualitative, describe surprisingly well the occurring diverse structural events and phase transitions in various lipid systems.

The amphiphilic property of lipids leads to self-aggregation in water solution, so that the hydrocarbon chains are segregated away from water, while the polar head groups are still residing in contact with water. Therefore, lipids form closed aggregates to prevent hydrocarbon–water contact, and the chemical free energy of the acyl chain is thereby minimized. This hydrophobic energy is proportional to the area of the hydrocarbon–water contact, having an interfacial hydrophobic free energy density of about 3.5×10^{-20} J nm^{-2}, which can be compared with the interfacial tension of an oil/water interface equal to about 5×10^{-20} J nm^{-2}. Furthermore, the distance of any methyl group of any acyl chain to the aggregate interface cannot be larger than the fully extended length of the hydrocarbon chain (usually the average chain length is about 0.7–0.8 times the all-trans length of the chain). This leads to that certain packing restrictions of the lipid molecules have to be fulfilled in the aggregates formed (Tanford, 1980; Israelachvili et al., 1980). A very useful concept for a qualitative understanding of the phase behavior in amphiphile systems is based on a consideration of the shape of the lipid molecules. According to Israelachvili et al. (1980), the self-assembly of lipid molecules depends on a dimensionless *packing parameter* defined by the ratio $v(al)^{-1}$, where v is the acyl chain volume, l is an average chain length, and a is the head-group area at the hydrocarbon–water interface. When the packing parameter is equal to unity (cylindrical-like molecules), there are optimal conditions for the formation of a bilayer structure. For $v(al)^{-1} > 1$ (Wieslander et al., 1980), the molecules are wedge-shaped, and the lipid monolayer prefers to curve toward the water region, and an H_{II} phase may form. Although this simple approach is very useful for qualitative considerations, it is difficult to use for more quantitative calculations, mainly due to the complex dependence of the area a on the temperature and concentration.

A different approach was taken by Gruner (1985), who used a concept [although related to the packing parameter $v(al)^{-1}$; see below] that has a more general character, namely, the so-called *spontaneous curvature*, H_0, of the lipid monolayer. This concept was first introduced by Helfrich (1973) for PC bilayer systems.

The total curvature free energy, G_{curve}, is given by (Helfrich, 1973)

$$G_{\text{curve}} = k_m(H - H_0)^2 + k'_m K \qquad (1)$$

where H is the local mean curvature of the monolayers [the mean curvature $H = (R_1^{-1} + R_2^{-1})/2$, where R_1 and R_2 are the principal radii], the Gaussian curvature $K = R_1^{-1}/R_2^{-1}$, k_m and $k_m{}'$ are elastic constants. Gruner and co-workers have shown that the energy of curvature plays a dominant role in the formation of H_{II} phases, where only the mean curvature has to be considered since K is equal to zero (since one of the principal radii is infinitely large). Thus, to minimize the free energy of curvature of an H_{II} phase, it is advantageous to have H close to H_0. However, for a phospholipid monolayer to form a cylinder of radius $R_0 = 1/H_0$, there will also be a nonzero packing energy (Gruner, 1985). For the cubic phases, on the other hand, the two principal radii are both finite, and the Gaussian curvature comes into play. However, several cubic phases have a topology that can be described by so-called periodic minimal surfaces, i.e., $H = 0$, which has been utilized in calculations of the stability of cubic phases (Anderson et al., 1988), although nothing is known about the Gaussian curvature in these systems.

Here we have used the convention that for a lipid monolayer $H > 0$ when it curves toward the hydrocarbon chain region and $H < 0$ when the layer curves toward the aqueous region. Finally, it should be mentioned that recently Hyde (1989) has shown that the packing parameter is related to the two curvatures in question by

$$v(al)^{-1} = 1 + Hl + (1/3)Kl^2 \qquad (2)$$

Obviously, it can be expected that the size of the polar head group and its interactions play important roles for the formation of a cubic or an H_{II} phase, where the smallest head groups should be in favor of an H_{II} phase and the cubic phase may form as an intermediate phase between the L_α and H_{II} phases. Therefore, usually the area of extension of a cubic phase in the phase diagram is rather small and limited (Lindblom & Rilfors, 1989).

The FTIR spectra obtained for the different parts of the polar head groups of MO and DOPC strongly indicate that there is a hydrogen-bond interaction between these molecular species. This hydrogen bonding contributes to a decrease in the mean interfacial surface area per lipid molecule, while the mean acyl chain volume can be considered as being constant. Thus, the effective shape of the molecules in a bilayer structure will change toward a more wedge-like geometry if MO or DOPC is added to the lamellar system, which eventually will lead to a phase transition to a nonlamellar structure. In terms of curvature, this means that the monolayer adopts an increasingly negative curvature as the amount of MO or DOPC increases in the MO/DOPC/water system. The first energy minimum will be reached when the lipid monolayer has a curvature such that it is draped on a surface, where every point is a saddle point ($K < 0$) and a cubic phase will form. However, MO forms cubic phases by itself in water which most probably is due to that the number of intramolecular hydrogen bonds decreases with increasing water concentration.

The experimental findings that the carbonyl group is less hydrated in the cubic than in the lamellar phase strongly support this interpretation. Thus, water penetrating into the lipid monolayer closer to the acyl region will lead to an increase in interfacial tension, which will be counteracted by a change toward a more negative curvature of the monolayer. The balance between the intramolecular hydrogen bonding and the formation of a negative curvature is very subtle. Thus, for example, addition of an alkane to a DOPC/water system (Sjölund et al., 1987, 1989) may result in the formation of an H_{II} phase, while the addition of MO to the same system leads to the formation of a cubic phase (Gutman et al., 1984). This strongly indicates that hydrogen bonding plays an important role in modifying the spontaneous curvature and the molecular packing of the lipid monolayer. It can therefore also be expected that at even higher water concentration of the MO/DOPC/water system a so-called L_3 phase might form. The monolayer curvature plays a dominant role in the formation of L_3 phases as described recently by Anderson et al. (1989). In particular, such phases are expected to form in systems containing nonionic lipids, were long-range Coulombic forces are absent. The search for this phase will be left to a later investigation.

CONCLUSIONS

The hydrogen bonding and hydration have been studied for the three systems MO/water, DOPC/water, and MO/DOPC/water. The most striking result is that the presence of DOPC in the latter system implies that the intramolecular hydrogen bonding in MO is broken and an intermolecular hydrogen bond with the polar head group of DOPC is formed. It is evident that the *sn*-3 OH group of MO competes with water to interact with the PO_2^- groups of DOPC. Furthermore, addition of MO to the DOPC/water system implies an increasing hydration of the ester carbonyl groups at the interfacial region of the lipid bilayer. Therefore, the system responds to this unfavorable increase in free energy by curling the lipid monolayer to prevent hydrocarbon–water contact. Similarly, attractive interactions between the polar head groups will lead to a change in the molecular shape to a more wedgelike geometry imposing a curling of the bilayer. Such changes will eventually lead to a phase transition to a nonlamellar phase.

Registry No. DOPC, 4235-95-4; MO, 25496-72-4; water, 7732-18-5.

REFERENCES

Anderson, D. M., Gruner, S. M., & Leibler, S. (1988) *Proc. Natl. Acad. Sci. U.S.A. 85*, 5364–5368.

Anderson, D., Wennerström, H., & Olsson, U. (1989) *J. Phys. Chem. 93*, 4243–4253.

Berde, C. B., Andersen, H. C., & Hudson, B. S. (1980) *Biochemistry 19*, 4279–4293.

Blume, A., Hübner, W., & Messner, G. (1988) *Biochemistry 27*, 8239–8249.

Boggs, J. M. (1987) *Biochim. Biophys. Acta 906*, 353–404.

Bush, S. F., Levin, H., & Levin, I. W. (1980) *Chem. Phys. Lipids 27*, 101–111.

Casal, H. L., & Mantsch, H. H. (1984) *Biochim. Biophys. Acta 799*, 381–401.

Finer, E. G., & Darke, A. (1974) *Chem. Phys. Lipids 12*, 1–16.

Gruner, S. M. (1985) *Proc. Natl. Acad. Sci. U.S.A. 82*, 3665–3669.

Gruner, S. M. (1989) *J. Phys. Chem. 93*, 7562–7570.

Gutman, H., Arvidson, G., Fontell, K., & Lindblom, G. (1984) in *Surfactants in Solution* (Mittal, K., & Lindman, B., Eds.) Vol. 1, pp 143–152, Plenum Press, New York.

Helfrich, W. (1973) *Z. Naturforsch., C: Biochem., Biophys., Biol., Virol. 28C*, 693–703.

Holmgren, A., Johansson, L. B.-Å., & Lindblom, G. (1987) *J. Phys. Chem. 91*, 5298–5301.

Holmgren, A., Lindblom, G., & Johansson, L. B.-Å. (1988) *J. Phys. Chem. 92*, 5639–5642.

Hope, M. J., & Cullis, P. R. (1981) *Biochim. Biophys. Acta 640*, 82–90.

Hyde, S. T. (1989) *J. Phys. Chem. 93*, 1458–1464.

Hyde, S. T., Andersson, S., Ericsson, B., & Larsson, K. (1984) *Z. Kristallogr. 168*, 213–218.

Jensen, J. W., & Schutzbach, J. S. (1984) *Biochemistry 23*, 1115–1119.

Jensen, J. W., & Schutzbach, J. S. (1988) *Biochemistry 27*, 6315–6320.

Jensen, J. W., & Schutzbach, J. S. (1989) *Biochemistry 28*, 851–855.

Johansson, L. B.-Å., & Lindblom, G. (1980) *Q. Rev. Biophys. 13*, 63–118.

Johansson, L. B.-opdA., & Lindblom, G. (1981) *Biophys. J. 36*, 735–741.

Johansson, L. B.-Å., Davidsson, Å., Lindblom, G., & Norden, B. (1978) *J. Phys. Chem. 82*, 2604–2609.

Johansson, L. B.-Å., Davidsson, Å., Lindblom, G., & Naqvi, R. (1979) *Biochemistry 18*, 4249–4253.

Johansson, L. B.-Å., Lindblom, G., Wieslander, Å., & Arvidson, G. (1981) *FEBS Lett. 128*, 97–99.

Israelachvili, J. N., Mitchell, D. J., & Ninham, B. W. (1976) *J. Chem. Soc., Faraday Trans 1, 72*, 1525–1568.

Kahn, A., Rilfors, L., Wieslander, Å., & Lindblom, G. (1981) *Eur. J. Biochem. 116*, 215–220.

Kawai, T., Umemura, J., & Takenaka, T. (1984) *Colloid Polym. Sci. 262*, 61–66.

LeNeveu, D. M., Rand, R. P., Parsegian, V. A., & Gingell, D. (1977) *Biophys. J. 18*, 209–230.

Lindblom, G., & Wennerström, H. (1977) *Biophys. Chem. 6*, 167–171.

Lindblom, G., & Rilfors, L. (1989) *Biochim. Biophys. Acta 988*, 221–256.

Lindblom, G., Lindman, B., & Tiddy, G. J. T. (1978) *J. Am. Chem. Soc. 100*, 2299–2303.

Lindblom, G., Larsson, K., Johansson, L., Fontell, K., & Forsen, S. (1979) *J. Am. Chem. Soc. 101*, 5465–5470.

Lindblom, G., Brentel, I., Sjölund, M., Wikander, G., & Wieslander, Å. (1986) *Biochemistry 25*, 7502–7510.

Lindblom, G., Sjölund, M., & Rilfors, L. (1988) *Liq. Cryst. 3*, 783–790.

Longley, W., & McIntosh, T. J. (1983) *Nature 303*, 612–614.

Lutton, E. S. (1965) *J. Am. Oil Chem. Soc. 42*, 1068–1070.

Lutz, H. D., Pobitschka, W., Frischemeimer, B., & Becker, R. A. (1978) *Appl. Spectrosc. 32*, 541–547.

Mantsch, H. H., Martin, A., & Cameron, D. G. (1981) *Biochemistry 20*, 3138–3145.

Mantsch, H. H., Cameron, D. G., Umemura, J., & Casal, H. L. (1984) *J. Mol. Struct. 60*, 263–268.

McIntosh, T. J., & Simon, S. A. (1986) *Biochemistry 25*, 4948–4955.

Mendelsohn, R., Dluhy, R. A., Crawford, T., & Mantsch H. H. (1984) *Biochemistry 23*, 1498–1504.

Nagle, J. F. (1976) *J. Membr. Biol. 27*, 233–250.

Nagle, J. F. (1980) *Annu. Rev. Phys. Chem. 31*, 157–195.

Navarro, J., Toivio-Kinnucan, M., & Racker, E. (1984) *Biochemistry 23*, 130–135.

Patton, J. S., & Carey, M. C. (1979) *Science 204*, 145–148.

Pearson, R. H., & Pascher, I. (1979) *Nature 281*, 499–501.

Persson, N.-O., & Lindblom, G. (1979) *J. Phys. Chem. 83*, 3015–3019.

Pimentel, G. C., & McClellan, A. L. (1960) *The Hydrogen Bond*, W. H. Freeman and Company, New York.

Rothschild, W. G. (1984) *Dynamics of molecular liquids*, John Wiley and Sons, New York.

Sarikov, G. N., Dashevsky, V. G., & Malenkov, V. G. (1974) *Mol. Phys. 27*, 1249–1269.

Seddon, J. M. (1990) *Biochim. Biophys. Acta 1031*, 1–69.

Siegel, D. P. (1986) *Chem. Phys. Lipids 42*, 279–301.

Siegel, D. P., Banschbach, J., & Yeagle, P. L. (1989) *Biochemistry 28*, 5010–5019.

Sjölund, M., Lindblom, G., Rilfors, L., & Arvidson, G. (1987) *Biophys. J. 52*, 145–153.

Sjölund, M., Rilfors, L., & Lindblom, G. (1989) *Biochemistry 28*, 1323–1329.

Sternin, E., Fine, B., Bloom, M., Tilcock, C. P. S., Wong, K. F., & Cullis, P. R. (1988) *Biophys. J. 54*, 689–694.

Tanford, C. (1980) *The Hydrophobic Effect*, 2nd, ed., Wiley, New York.

Teissié, J., Prats, M., Soucaille, P., & Tocanne, J. F. (1985) *Proc. Natl. Acad. Sci. U.S.A. 82*, 3217–3221.

Tilcock, C. P. S., & Fisher, D. (1982) *Biochim. Biophys. Acta 685*, 340–346.

Tocanne, J. F., & Teissé, J. (1990) *Biochim. Biophys. Acta 1031*, 111–142.

Turmond, R., & Brown, M. F. (1991) *Biophys. J.* (in press).

Umemura, J., Cameron, D. G., & Mantsch, H. H. (1980) *J. Chem. Phys. 84*, 2272–2277.

Umemura, J., Mantsch, H. H., & Cameron, D. G. (1981) *J. Colloid Interface Sci. 83*, 558–568.

Wieslander, Å., Christiansson, A., Rilfors, L., & Lindblom, G. (1980) *Biochemistry 19*, 3650–3655.

Wieslander, Å., Rilfors, L., Johansson, L. B.-Å., & Lindblom, G. (1981) *Biochemistry 20*, 730–735.

Wong, P. T. T., & Mantsch, H. H. (1988) *Chem. Phys. Lipids 46*, 213–224.

Zundel, G. (1969) *Hydration and Intermolecular Interaction*, Academic Press, London.